Proc. Int. Symp. "Brittle Matrix Composites 8"
A.M. Brandt, V.C. Li and I. H. Marshall, eds.
Warsaw, October 23-25, 2006
ZTUREK RSI and Woodhead Publ., Warsaw 2006

FLEXURAL RESPONSE OF REINFORCED BEAM WITH HIGH DUCTILITY CONCRETE MATERIAL

Maria M. SZERSZEN*, Aleksander SZWED**, and Victor C. LI*
*Department of Civil and Environmental Engineering, University of Michigan, USA
e-mail: mariasz@umich.edu, vcli@umich.edu
**Civil Engineering Faculty, Warsaw University of Technology, Poland
e-mail: a.szwed@il.pw.edu.pl

ABSTRACT

This paper reports on a study of flexural behavior of steel reinforced ductile engineered cementitious composite (ECC) members. ECC materials show extraordinary levels of strain ductility in tension (2-4%). Multiple micro-cracking in ECC delays fracture localization typically observed in normal concrete. Based on experimental stress-strain curves for ECC and reinforcing steel, a typical elastic-plastic model is assumed to derive the moment-curvature relation for reinforced beams in flexure. The resulting closed-form formulas are used in prediction of ultimate flexural capacity and ductility of beams made of ECC. Substantial difference in beams performance shows beneficial features of ductile ECC material. Direct design examples for beams and slabs using ductile or brittle materials present quantitative comparison of flexural behavior of structural members for typical design cases.

Keywords
Composites, strain-hardening, fibers, ductility, ECC, RC, flexure

INTRODUCTION

Ductile engineered cementitious composite is characterized by an ability to sustain equal or higher levels of loading after first cracking, while straining is significantly higher than the elastic limit. The high strain ductility can be achieved by controlling the composite ingredients of fiber, matrix and interface so that cracks initiated from defect zones do not result in fracture localization [1]. Instead, the bridging fibers transfer the tensile load back into the matrix to create additional microcracks. One such ECC material extensively studied contains 2% of PolyVinyl Alcohol (PVA) fibers of $40\,\mu m$ in diameter and $12\,mm$ long have been demonstrated to achieve strain ductility exceeding 3% under uniaxial tension [1,2]. During tensile straining of a ECC specimen, steady state crack propagation occurs with multiple dense cracking developing, and preserving stable crack opening at about $60\,\mu m$. Typical experimental stress-strain curves in uniaxial tensile test are shown in Fig.1. The experimental curves show a non-softening trend with strain capacity over 300 times that of a non-reinforced concrete matrix.

Application of a new type of high performance material in engineering practice requires extensive analysis of the structural members response in order to develop design guidelines. The high ductility and tight crack width features of ECC is expected to provide

significant advantages in ultimate and serviceability limit states of structural members under tensile or flexural loading. Full benefits of such material, such as increased moment or shear capacity of structural members, can be addressed in design procedures using a material model different from that established for ordinary concrete.

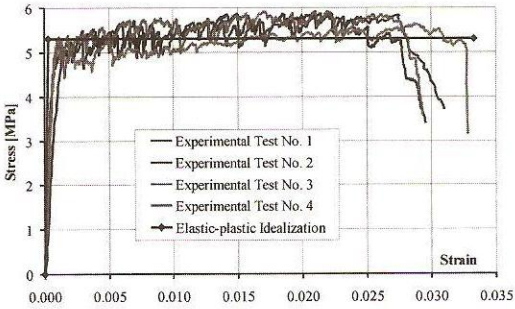

Fig.1. Typical experimental stress-strain curves for ECC in uniaxial direct tension test.

In this paper, flexural analysis of reinforced ECC slender beams is presented. Utilizing available uniaxial tension and compression tests results for ECC, as well as properties of reinforcing steel, a simple idealization of stress-strain curves is assumed. Using strain compatibility and constitutive relationships of constituent materials, closed-form formulas for moment-curvature relations are derived. Closed-form formulas are used in prediction of ultimate flexural capacity and curvature ductility of reinforced beams made of ECC, and they are very useful in parametric study. Comparison of designs performed for ductile ECC and ordinary brittle concrete highlights beneficial properties of ECC when used in structural members under flexural loading.

BASIC ASSUMPTIONS

Based on experimental stress-strain curves for uniaxial tension (Fig.1) and uniaxial compression tests for ECC, some idealizations and simplifications in material descriptions were carried out. Linear elastic and then perfectly plastic one-dimensional material model was assumed because of its simplicity and easy application. The behavior of ECC is defined as,

$$\sigma = \begin{cases} -\sigma_{0C} & \text{for} \quad -\varepsilon_{UC} \le \varepsilon < -\varepsilon_{0C} \\ E_c \varepsilon & \text{for} \quad -\varepsilon_{0C} \le \varepsilon \le \varepsilon_{0T} \\ \sigma_{0T} & \text{for} \quad \varepsilon_{0T} < \varepsilon \le \varepsilon_{UT}, \end{cases} \tag{1}$$

where ε_{0C} and ε_{0T} are elastic limit strain in compression and tension, σ_{0C} and σ_{0T} are the elastic limit stress in compression and tension. Elastic (Young's) modulus for linear elastic range is defined by formulas, $E_c = \sigma_{0C} / \varepsilon_{0C} = \sigma_{0T} / \varepsilon_{0T}$. Ultimate strains in tension and compression, ε_{UT} ε_{UC} are defined to control stable straining of material.

The behavior of reinforcing steel is assumed to be linear elastic and then perfectly plastic, and is defined by the following relationship,

$$\sigma_S = \begin{cases} -f_Y & \text{for} \quad -\varepsilon_U \le \varepsilon_S < -\varepsilon_Y \\ E_s \varepsilon_S & \text{for} \quad -\varepsilon_Y \le \varepsilon_S \le \varepsilon_Y \\ f_Y & \text{for} \quad \varepsilon_Y < \varepsilon_S \le \varepsilon_U, \end{cases} \tag{2}$$

where ε_Y is elastic limit strain, f_Y is elastic limit (yield) stress, $E_s = f_Y/\varepsilon_Y$ is elastic modulus for steel in linear elastic range. The ultimate strain in reinforcing steel ε_U is typically several times larger than the ultimate tensile strain in ECC, and this parameter will not be critical in the performed analysis.

Assumption of plane cross-section of a beam is adopted in the following derivation of basic equation for bending of slender beams. The assumption states that beam cross-section remains plane in any stage of beam deformation. Neutral axis (or generally a curve) is defined as the position of points of a beam's cross-section where no axial strains and stresses occur, and its vertical displacement is given by the function $w(x)$. According to the assumption, the horizontal displacement, u, of a point in distance of z from the neutral axis is expressed as,

$$u(x,z) = -z\frac{\mathrm{d}w(x)}{\mathrm{d}x} = -z\,\mathrm{tg}\phi \cong -z\phi(x). \tag{3}$$

Then, the axial strain is defined as,

$$\varepsilon(x,z) = \frac{\partial u(x,z)}{\partial x} = -z\frac{\mathrm{d}^2 w(x)}{\mathrm{d}x^2} = z\kappa(x), \tag{4}$$

where $\kappa(x)$ is the curvature of a bent beam, and $\phi(x)$ is the slope. The relation between axial strain and curvature given by (4) is often called the strain compatibility.

MOMENT-CURVATURE RELATION FOR SECTION

The moment-curvature relationship for cross-section is determined by considering compatibility conditions of the section, (4), and the stress-strain relations of the constituent materials (1) and (2). For simplicity, a rectangular cross-section with single layer of reinforcement will be assumed in the following analysis, but presented approach can be applied to any symmetrical cross-sections with multiple layers of reinforcement. Perfect bond between reinforcing steel and ECC is assumed, what is experimentally observed [4]. Assuming pure bending, derivation of the moment-curvature relationship involves the assumption of various levels of strains in the cross-section, corresponding to the different stages of loading. Stress distribution defined according to the constitutive low is integrated over the cross-section area. Zero axial force condition defines the compression zone depth, which subsequently is used to obtain the moment capacity of the cross-section.

The complete moment-curvature relationship is subdivided onto five phases depending on the load level and reinforcement ratio. Phase I is determined by the linear elastic behavior of constituent materials in the cross-section. Phase II is defined with the assumption of elastic-plastic behavior of ECC in the tension zone, and elastic behavior in the compression zone, while steel is in elastic range. Phase III, with elastic-plastic behavior of ECC in the tension zone, and elastic behavior in the compression zone; steel reaches yield stress. Phase IV, valid only for high reinforcement ratios, covers elastic-plastic behavior of ECC material in both, tension and compression zones, while steel is in elastic range. Phase V occurs with elastic-plastic behavior of ECC material in both, tension and compression zones, and steel is plastic. The basic idea of the proposed phase subdivision is explained in Fig.2, and Fig.3, what summarizes the analysis performed in this section. In the following derivations, each phase is considered separately and closed-form solutions for moment-curvature relations are obtained. Limits of application for each phase are defined, and some characteristic values of moment and curvature are given. Formulas for other parameters involved, such as: the depth of compression zone, and cracking and crushing zone depths are also given.

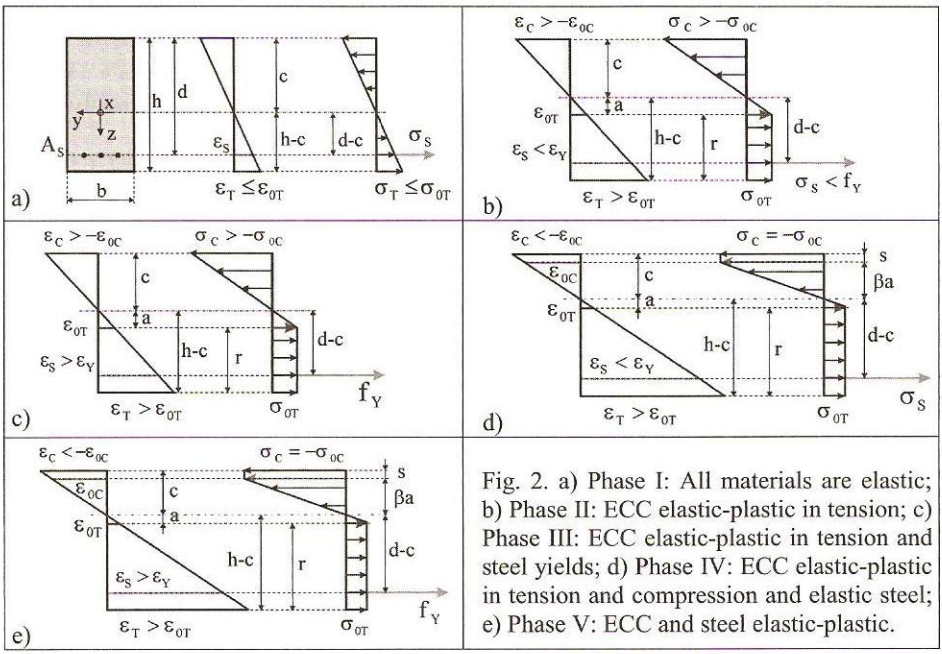

Fig. 2. a) Phase I: All materials are elastic; b) Phase II: ECC elastic-plastic in tension; c) Phase III: ECC elastic-plastic in tension and steel yields; d) Phase IV: ECC elastic-plastic in tension and compression and elastic steel; e) Phase V: ECC and steel elastic-plastic.

Phase I.

In the case of strains and stresses linearly distributed in beam cross-section (Fig.2a), the moment-curvature relationship and compression zone depth, c, can be expressed as,

$$m_I = \left\{ \frac{1}{1+\xi} + \frac{4\xi}{1+\xi}\left[1-3\delta(1-\delta)\right] \right\} k_I, \qquad c_I = \frac{1+2\xi\delta}{2(1+\xi)} h, \tag{5}$$

where scaled moment $m = M / M_{cE}$ and curvature $k = \kappa / \kappa_{cE}$ are used throughout this analysis. The elastic limit curvature, κ_{cE}, and moment, M_{cE}, for an un-reinforced rectangular ECC cross-section are given by formulas,

$$\kappa_{cE} = \frac{2\varepsilon_{0T}}{h} = \frac{2\sigma_{0T}}{hE_c} \qquad \text{and} \qquad M_{cE} = \frac{bh^2}{6}\sigma_{0T} \tag{6}$$

The elastic bending stiffness of an un-reinforced beam is then: $E_c I_c = M_{cE} / \kappa_{cE}$. The dimensionless parameters ρ, ξ and δ in (5) stand for reinforcement ratio, modular-reinforcement ratio and effective depth ratio, respectively:

$$\rho = \frac{A_S}{bh}, \qquad \xi = \rho \frac{E_S}{E_c} = \rho n, \qquad \text{and} \qquad \delta = \frac{d}{h}, \tag{7}$$

Further notation is explained in Fig. 2. The actual moment, M, and actual curvature, κ, in (5) are lower than the elastic limits in phase I. The end of elastic behavior of the cross-section is reached when in exterior fibers of beam tensile stresses are equal to the elastic limit stress σ_{0T}. Elastic limit curvature and moment of reinforced cross-section are,

$$k_E = \frac{1+\xi}{1+2\xi(1-\delta)}, \qquad m_E = \frac{1+4\xi\left[1-3\delta(1-\delta)\right]}{1+2\xi(1-\delta)}. \tag{8}$$

Phase II.

Phase II of cross-sectional behavior begins when strains in the ECC matrix exceed the elastic limit, ε_{0T}, in the tension zone (Fig.2b). The condition of zero axial force yields to the evaluation of depth of the compression zone, c, and then cracking zone depth r:

$$c_{II} = \left[\sqrt{\xi(2\delta+\xi)+\frac{1+\xi}{k}} - \frac{1}{2k} - \xi\right]h, \qquad r_{II} = \left(1-\frac{1}{2k}\right)h - c_{II}. \tag{9}$$

The moment-curvature relationship can be expressed as follows,

$$m_{II} = 3+6\xi(1+\xi+\delta)+4\xi\left[2\xi^2+3\delta(\delta+2\xi)\right]k - 2\left[1+\xi+4\xi(2\delta+\xi)k\right]\sqrt{\xi(2\delta+\xi)+\frac{1+\xi}{k}}. \tag{10}$$

When the elastic limit stress in steel, f_Y, is reached, the end of elastic behavior of steel defines the end of the phase. Using the ratio, $\gamma = \varepsilon_Y / \varepsilon_{0T}$, the corresponding curvature is,

$$k_{YT} = \frac{1+\gamma\xi+\delta(\gamma-1)+\sqrt{(1+\gamma\xi)\left[1+\gamma\xi+2\delta(\gamma-1)\right]}}{2\delta^2}. \tag{11}$$

In the case of highly reinforced cross-section, the end of elastic behavior of ECC in compression region can be reached, before steel starts to yield. At this stage of loading, compressive stress in external fibers is σ_{0C}, and using parameter $\beta = \sigma_{0C} / \sigma_{0T}$, the curvature is,

$$k_{0CC} = \frac{\beta\xi - 1 + \sqrt{2(1+\beta)^2\delta\xi + (\beta\xi-1)^2}}{4\delta\xi}. \tag{12}$$

Balance point (see Fig.3, point B), reflecting simultaneously reached limits, f_Y for steel and σ_{0C}, for concrete, can be evaluated comparing (11) and (12). The balance point reinforcement ratio, ξ_B, curvature and moment for this point are given by the formulas,

$$\xi_B = \frac{\delta(1+\beta)^2}{2\gamma(\gamma+\beta)} - \frac{1}{\gamma} = n\rho_B, \quad k_B = \frac{\beta+\gamma}{2\delta}, \quad m_B = 3(1-2\delta)+(2\beta+3\gamma-1)\left[\frac{(1+\beta)\delta}{\beta+\gamma}\right]^2. \tag{13}$$

Phase III.

Phase III governs when tensile strains in concrete composite are greater then elastic limit, ε_{0T}, in a part of beam cross-section, and reinforcing steel yields in tension, whereas concrete remains elastic in compression, see Fig.2c. This case is typical for tensile controlled failure path of a cross-section. The compression zone depth, c, and moment-curvature relationship is then as follows:

$$c_{III} = \left[\sqrt{\frac{1+\gamma\xi}{k}} - \frac{1}{2k}\right]h, \qquad m_{III} = 3(1+2\delta\gamma\xi) - 2(1+\gamma\xi)\sqrt{\frac{1+\gamma\xi}{k}}. \tag{14}$$

The end of elastic behavior in compression is reached when compressive stress in exterior fibers is equal to σ_{0C}. Then, the curvature and moment for the end of the phase III are,

$$k_{0C} = \frac{(1+\beta)^2}{4(1+\gamma\xi)}, \qquad m_{0C} = 3(1+2\gamma\delta\xi) - \frac{4(1+\gamma\xi)^2}{1+\beta}. \tag{15}$$

Phase IV.

In phase IV, strains are greater then elastic limit in tension, ε_{0T}, and in compression, strains are greater then elastic limit in compression, ε_{0C}, while reinforcing steel remains in the elastic range. This case is appropriate for compression controlled failure path of a cross-section. Axial force and bending moment can be calculated using stress diagram shown in Fig.2d. The compression zone depth, c, and crushing zone depth, s, can be obtained as,

$$c_{IV} = \frac{\beta^2 - 1 + 4k(1+2\delta\xi k)}{4k(1+\beta+2\xi k)}h, \qquad s_{IV} = c_{IV} - \frac{\beta}{2k}h, \tag{16}$$

while moment-curvature formula can be expressed as

$$m_{IV} = 3\left[(1-\delta)^2 + \beta\delta^2\right] - \frac{(1+\beta)^3}{4k^2} + \frac{3(\beta-1)^2(1+\beta)^3}{16k^2(1+\beta+2\xi k)^2} - \frac{3(1+\beta)[1-\delta(1+\beta)]^2}{(1+\beta+2\xi k)^2} + \frac{3\xi(\beta^2-1)[1-\delta(1+\beta)]}{(1+\beta+2\xi k)^2} + \frac{3\xi(\beta^2-1)^2}{4k(1+\beta+2\xi k)^2}. \tag{17}$$

When yield stress in steel, f_Y, is reached, the end of phase IV occurs, and curvature is,

$$k_{YC} = \frac{(1+\beta)(\beta-1+2\gamma)}{4\left[(1+\beta)\delta - (1+\gamma\xi)\right]}. \tag{18}$$

Another possible end of this phase occurs, when the end of concrete composite ductility in compression, ε_{UC}, is reached before steel starts yielding. Then, introducing $\lambda = \varepsilon_{UC} / \varepsilon_{0C}$, the value for curvature is,

$$k_{UCC} = \frac{\beta\lambda\xi - 1 + \sqrt{2\delta\xi(1+\beta)[1+\beta(2\lambda-1)] + (\beta\lambda\xi - 1)^2}}{4\delta\xi}. \tag{19}$$

Simultaneous reaching of ε_{UC} in concrete composite and f_Y in steel can be derived by comparing (18) and (19), (see Fig.3, point C). Then the reinforcement ratio for this state is,

$$\xi_C = \frac{\delta - 2\gamma - 2\beta\lambda(1-\delta) + (2\lambda-1)\delta\beta^2}{2\gamma(\gamma+\beta\lambda)} = n\rho_C, \tag{20}$$

and the characteristic values of curvature and moment are given by the formulas,

$$k_C = \frac{\beta\lambda+\gamma}{2\delta}, \qquad m_C = 3\left[(1-\delta)^2 + \beta\delta^2\right] - \frac{(1+\beta)\delta^2\left[1+\beta^2+3\gamma(\gamma-1)+\beta(3\gamma-1)\right]}{(\beta\lambda+\gamma)^2}. \tag{21}$$

Phase V.

In the case of strains in compression greater then ε_{0C}, and stress in steel equal to f_Y, phase V of cross-sectional behavior occurs, Fig.2e. The depth of compression zone and moment-curvature are,

$$c_V = \left[\frac{1+\gamma\xi}{1+\beta} + \frac{\beta-1}{4k}\right]h, \qquad m_V = \frac{3\beta}{1+\beta} + 6\gamma\delta\xi - \frac{3\gamma\xi(2+\gamma\xi)}{1+\beta} - \frac{(1+\beta)^3}{16k^2}. \tag{22}$$

When ultimate strains, ε_{UC}, are reached, the ultimate curvature and moment are,

$$k_{UC}=\frac{(1+\beta)[1+(2\lambda-1)\beta]}{4(1+\gamma\xi)},\qquad m_{UC}=\frac{3\beta}{1+\beta}+6\gamma\delta\xi-\frac{3\gamma\xi(2+\gamma\xi)}{1+\beta}-\frac{(1+\beta)(1+\gamma\xi)^2}{[1+(2\lambda-1)\beta]^2},\tag{23}$$

For a very lightly reinforced section, compression failure mode controls the ultimate strain capacity when the strain ratios, λ, and $\alpha=\varepsilon_{UT}/\varepsilon_{0T}$, fulfill the following inequality,

$$\lambda<\frac{1}{2}+\frac{2\alpha-1}{2\beta^2}=\lambda_{Bal},\tag{24}$$

where λ_{Bal} is the balanced strain capacity failure factor, reflecting simultaneous reaching of strain ductility of ECC in tension and compression. In cases other than (24), tension failure mode controls sectional failure. Then, the ultimate curvature and moment are as follows,

$$k_{UT}=\frac{(1+\beta)(2\alpha-1+\beta)}{4(\beta-\gamma\xi)},\qquad m_{UT}=\frac{3\beta}{1+\beta}+6\gamma\delta\xi-\frac{3\gamma\xi(2+\gamma\xi)}{1+\beta}-\frac{(1+\beta)(\beta-\gamma\xi)^2}{(2\alpha-1+\beta)^2}.\tag{25}$$

Tension point (see Fig.3, point *T*), for simultaneous reaching ultimate strains in compression and tension in ECC material, can be evaluated by comparing (23) and (25). Then, *T* point reinforcement ratio (for $\lambda<\lambda_{Bal}$), curvature and moment can be expressed as,

$$\xi_T=\frac{1-\beta^2-2(\alpha-\beta^2\lambda)}{2\gamma(\alpha+\beta\lambda)}=n\rho_T,\quad k_T=\frac{\alpha+\beta\lambda}{2},\quad m_T=\frac{3\beta}{1+\beta}+6\gamma\delta\xi-\frac{3\gamma\xi(2+\gamma\xi)}{1+\beta}-\frac{(1+\beta)^3}{4(\alpha+\beta\lambda)^2}.\tag{26}$$

Asymptotic ultimate capacity of reinforced ECC cross-section is reached when $\kappa\to\infty$. Then, the estimation of ultimate bending moment and depth of compression zone give values,

$$m_U=\frac{3\beta}{1+\beta}+6\gamma\delta\xi-\frac{3\gamma\xi(2+\gamma\xi)}{1+\beta},\qquad c_U=\frac{1+\gamma\xi}{1+\beta}h.\tag{27}$$

In Fig.3, the relationship between moment and curvature with explanation of notation used in foregoing derivations is shown. Curvature and moment are scaled by elastic limits (6), defined for an un-reinforced ECC cross-section. All characteristic parameters for curvature and moment are plotted for the five phases of behavior previously described and discussed. In phase I, moment-curvature relationship is linear, while in other phases II, III, IV and V is nonlinear. Four moment curvature relationships for characteristic reinforcement ratios $\rho=0$, ρ_T, ρ_B, ρ_C are plotted. Boundaries between phases are also plotted in Fig.3 with given characteristic strain in concrete or steel, related to the appropriate limit.

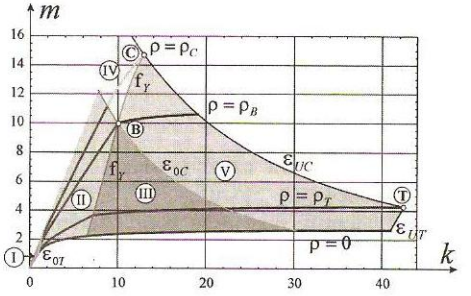

Fig. 3. Subdivision of moment-curvature relationship onto five phases in function of reinforcement ratio with identification of characteristic boundaries and points, where $m=M/M_{cE}$ and $k=\kappa/\kappa_{cE}$.

ANALYSIS OF RESULTS AND PARAMETRIC STUDY

In this section, basic analysis of moment-curvature relations and graphical interpretation of results are presented. Typical data for constituent materials are assumed and characteristic parameters involved in the model are obtained. Parametric study is mainly focused on the influence of reinforcement ratio, as well as on moment and curvature capacity for beams cross-section.

Based on experimental uniaxial compression and tension tests for ECC composite, characteristic strain and stress values have been estimated and used in the following calculations. Compressive strength and modulus of elasticity are estimated as: $f'_c = 60\,MPa$,. Tensile strength of concrete is: $\sigma_{0T} = 5.3\,MPa$, and structural compressive strength is assumed to be: $\sigma_{0C} = 0.88 f'_c = 53\,MPa$. Characteristic values for elastic limit strains are calculated as: $\varepsilon_{0T} = \sigma_{0T} / E_c = 0.0003$ and $\varepsilon_{0C} = \sigma_{0C} / E_c = 0.003$. Ultimate compressive and tensile strains are estimated as: $\varepsilon_{UC} = 0.0045$ and $\varepsilon_{UT} = 0.033$. Based on these values, basic dimensionless material parameters can be obtained: $\beta = \sigma_{0C} / \sigma_{0T} = 10$, $\lambda = \varepsilon_{UC} / \varepsilon_{0C} = 1.5$, and $\alpha = \varepsilon_{UT} / \varepsilon_{0T} = 110$. Properties of reinforcing steel are: $E_s = 200\,GPa$, $f_Y = 420\,MPa$ and $\varepsilon_Y = 0.00021$. Then, $n = E_s / E_c = 11.4$ and $\gamma = \varepsilon_Y / \varepsilon_{0T} = 7.0$ can be calculated. For this study, concrete cover ratio is assumed to be: $\delta = 0.85$. Balanced failure factor is $\lambda_{Bal} = 1.6$, which defines compression controlled failure for lightly reinforced cross-sections. Reinforcement ratios for characteristic points are: $\rho_B = 2.54\%$, $\rho_C = 4.34\%$.

The relationship between moment and curvature for several reinforcement ratios is shown in Fig. 4, where characteristic boundaries and points are explained. Characteristic values of curvatures and moments are: $\kappa_B = 10.00\,\kappa_{cE}$, $M_B = 10.00 M_{cE}$, $\kappa_C = 12.94\,\kappa_{cE}$, $M_C = 14.73 M_{cE}$. For the given material data, $\lambda < \lambda_{Bal}$, the compression controlled failure occurs for un-reinforced cross-section, without T point in Fig.4. Ultimate capacities of curvature and moment for un-reinforced cross-section are: $k_{UC} = 57.75$, $m_{UC} = 2.70$.

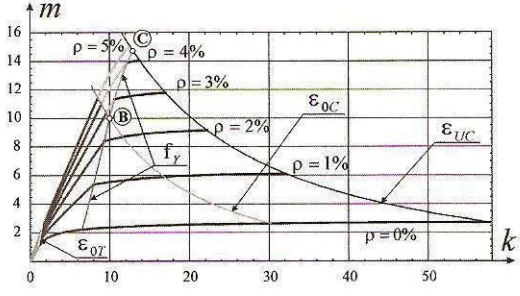

Fig. 4. Moment-curvature curves for several reinforcement ratios.

From the figure, it is easy to read an increase in moment capacity due to amount of reinforcement applied, as well as decrease in curvature ductility as a function of reinforcement ratio. Curves given in Fig. 4 clearly identify that there is no sudden drop in moment capacity after the first cracking. A sudden drop in moment capacity is typical for ordinary concrete, especially for lightly reinforced sections [3]. In case of ECC matrix applied in reinforced beam, moment-curvature curves indicate hardening behavior in the full range of curvatures, up to ultimate capacity. This occurs because of the continued tensile load carrying capacity of the ECC material, beyond its elastic limit.

The compression zone depth as a function of curvature and reinforcement ratio is presented in Fig.5a. Rapid decrease of compression zone in the cross-section is observed in phases II, III and V, for lightly reinforced sections. For highly reinforced sections, compression zone remains on relatively constant level with low curvature ductility, which is characteristic of sudden compression failure mode. In Fig.5b, cracking zone in tension and crushing zone in compression, are plotted as a function of curvature. In phase II, rapid development of cracking zone is observed. In phases III, IV and V, development of cracking zone is not as rapid as in phase II, and stabilizes for highly reinforced sections. Crushing zone develops rapidly for highly reinforced sections, especially in phase IV, what reflects brittle failure mode.

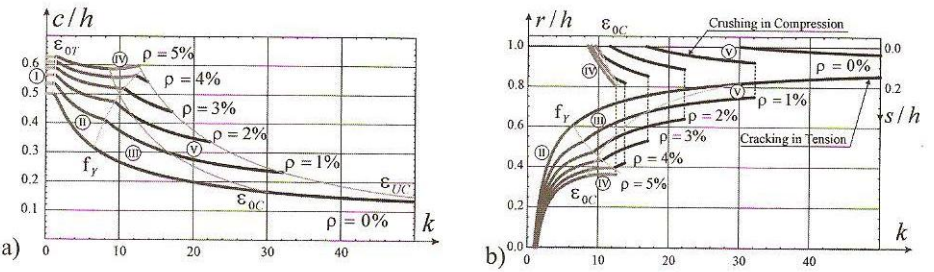

Fig. 5. a) Compression zone depth; b) Cracking and crushing zones development.

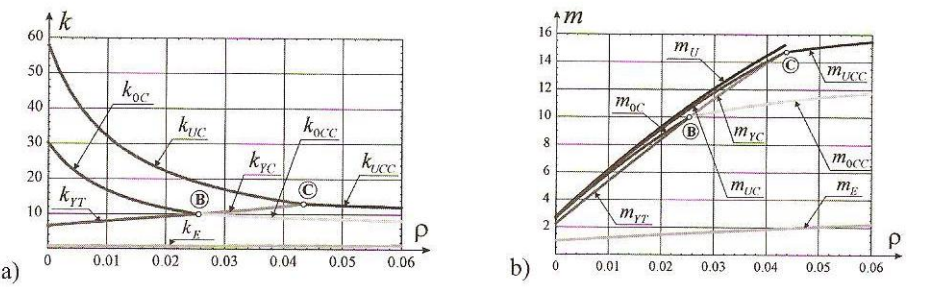

Fig. 6. Characteristic curvatures (a) and moments (b) as functions of reinforcement ratio.

Relationships between reinforcement ratio and characteristic curvatures, and corresponding moments are shown in Fig. 6. Fig.6a shows a decrease in curvature capacity (ductility) due to the amount of reinforcement applied. Different trends for characteristic curvatures can be observed for different curves. Elastic limit and ultimate ductility of ECC in compression decreases in hyperbolic manner with an increase of reinforcement ratio. These limits typically govern design in structural applications, when tension controlled failure (ductile) is a desired behavior for a structural member at ultimate load. Fig.6b shows an increase in moment capacity due to the amount of reinforcement in the cross-section. It can be observed, that the moment increase is close to linear for all phases of cross-section behavior. Two characteristic points, *B* and *C*, initiate deviations in the trend of moment increase. However, there is very little increase in elastic capacity due to reinforcement increase.

DESIGN EXAMPLES FOR BEAM WITH ECC AND ORDINARY CONCRETE

Moment capacity is calculated for two beams, made of ordinary concrete and ECC, with identical cross-section and reinforcement equal to maximum reinforcement permitted by ACI 318 Code, to enforce ductile failure mode. This maximum reinforcement should be no more that $0.75\rho_b$, where ρ_b is the balance failure percentage of reinforcement equal to 4.74% for ordinary concrete beam, and 5% for ECC beam. Compressive strength, equal to $f_c' = 8700\ psi\ (60\ MPa)$ is the same for OC and ECC material; reinforcing steel with yielding strength of $f_y = 60{,}000\ psi\ (Grade\,60)$ is used in both beams.

For the design calculation below, the percentage of reinforcement used in both beams, ρ, is assumed equal to,

$$\rho = 0.75 \times 0.0474 = 0.035\ (3.5\%)$$

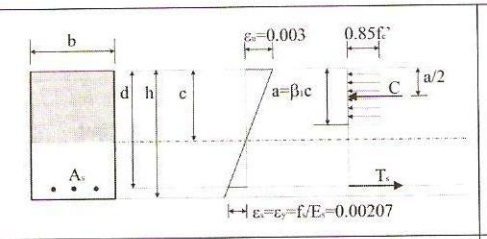

Fig. 7. Distribution of strains and stresses in the cross-section of single reinforced ordinary concrete beam.

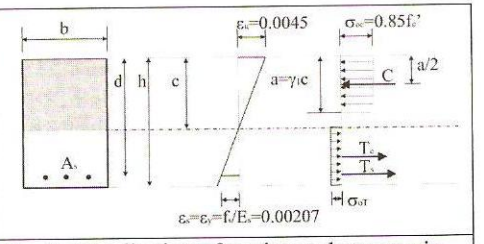

Fig. 8. Distribution of strains and stresses in the cross-section of single reinforced ECC beam.

Moment capacity of ordinary concrete beam (Fig. 7), calculated according to ACI 318 Code standard procedure is as follows,

$$C = 0.85 f_c' \times a \times b$$

$$T_s = A_s f_y$$

$$C = T_s \ \Rightarrow\ a = \frac{A_s f_y}{0.85 f_c' \times b}$$

$$A_s = 0.035 \times b \times d = 0.035 \times 15 \times 18.5 = 9.71 in^2$$

$$a = \frac{9.71 \times 60000}{0.85 \times 8700 \times 15} = 5.25 in$$

$$M_{cap_{OC}} = A_s f_y \left(d - \frac{a}{2} \right) = 9.71 \times 60000 \left(18.5 - \frac{5.25}{2} \right) = 9{,}248{,}775\ lb - in$$

Calculation of moment capacity of ECC beam presented below is modified comparing to standard code procedure, to account for strain and stress capacity of the composite in tension zone (Fig. 8). Stress block parameter, β_1, for ordinary concrete equal to 0.65 (for $f_c' = 8700\ psi$), is recalculated for ECC material, and becomes $\gamma_1 = 0.66$.

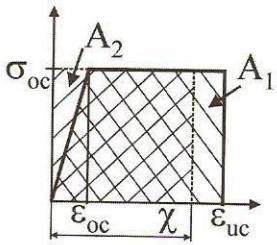

$A_1 = \sigma_{oc} \times \varepsilon_{oc} \times 0.5 + (\varepsilon_{uc} - \varepsilon_{oc})\sigma_{oc}$ $\qquad \varepsilon_{oc} = \dfrac{\sigma_{oc}}{E_c} = 0.00303$

$A_2 = \sigma_{oc} \times \chi$

$A_1 = A_2$

$$\chi = \frac{\sigma_{oc} \times \varepsilon_{oc} \times 0.5 + (\varepsilon_{uc} - \varepsilon_{oc})\sigma_{oc}}{\sigma_{oc}} = 0.00303 \times 0.5 + (0.0045 - 0.00303) = 0.00299$$

$$\gamma_1 = \frac{\chi}{\varepsilon_{uc}} = \frac{0.00299}{0.0045} = 0.66$$

$a = \gamma_1 c = 0.66c$

$A_s = 9.71 in^2$

$C = 0.85 f_c' ab$

$T_c = \sigma_{oT}(h-c)b$

$T_s = A_s f_y$

$C = T_c + T_s$

$$0.85 f_c' \times 0.66b \times c = \sigma_{oT}(h-c)b + A_s f_y \Rightarrow c = \frac{\sigma_{oT} hb + A_s f_y}{0.85 f_c' \times 0.66b + \sigma_{oT} b}$$

$$c = \frac{770 \times 20 \times 15 + 9.71 \times 60000}{0.85 \times 8700 \times 0.66 \times 15 + 770 \times 15} = 9.6 in$$

$a = 0.66 \times 9.6 = 6.3 in$

$$M_{cap} = T_c\left(\frac{h-c}{2} + c - \frac{a}{2}\right) + T_s\left(d - \frac{a}{2}\right)$$

$$M_{cap} = \sigma_{oT}(h-c)b\left(\frac{h-c+2c-a}{2}\right) + A_s f_y\left(d - \frac{a}{2}\right) = \frac{1}{2}\left[\sigma_{oT}(h-c)(h+c-a)b + A_s f_y(2d-a)\right]$$

$$M_{cap_{ECC}} = \frac{1}{2}\left[770(20-9.6)(20+9.6-6.3)15 + 9.7 \times 60000(2 \times 18.5 - 6.3)\right] = 10,342,308 lb-.$$

$$\frac{M_{cap_{ECC}}}{M_{cap_{OC}}} = 1.12$$

There is 12% increase in moment capacity for a beam made with ECC material if compared to the same, but made of ordinary concrete. The sensitivity analysis presented earlier show that the significance of ECC contribution in tensile zone increases for lower percentages of reinforcement. If similar comparison of moment capacities is performed for concrete bridge slabs with small amount of reinforcement ($\rho \cong 0.003\ (0.3\%)$ for empirical design), the difference in moment capacities is even more significant. Standard thickness ($7.5in$) ECC bridge deck indicates 230% increase in moment capacity if compared to the same, but ordinary concrete deck.

SUMMARY AND CONCLUSIONS

High ductility and stable multiple crack development in ECC gives a beneficial behavior in flexure of structural members made of this material. Simplified material models for the constituent materials in terms of stress-strain curves, allow for derivation of the analytical moment-curvature relations for beam. The resulting complete, closed-form formulas can be easily used for predicting the ultimate flexural capacity and curvature ductility of beams made of reinforced ECC. The resulting formulas are very useful in developing reliable design procedures for ECC, to aid structural engineers in applying such materials in field applications. The proposed rational derivation of moment-curvature relations gives qualitative and quantitative description of flexural behavior of reinforced ECC cross-section. The results can be applied to any beam or one-way slab, and extended to two-way slabs. Precisely defined phases in sectional behavior, and limits of application, can serve as a design guide for flexural elements.

From the present analyzes, a distinct difference between reinforced ECC (RECC) and common reinforced concrete can be observed. The sudden drop in moment capacity typical in ordinary concrete, especially for lightly reinforced sections, is absent when ECC is applied in reinforced beam. Moment-curvature curves indicate hardening behavior in whole range of curvatures, up to ultimate capacity. Although the modulus of elasticity for ECC is about 20-25% lower than for ordinary concrete with the same compressive strength, the flexural stiffness (in post cracked phase II) of reinforced cross-section is of the same order as for RC, and even higher for lightly reinforced sections. The ultimate flexural capacity is always higher for RECC than for RC, especially when low reinforcement ratio is applied. For instance, for $\rho = 1\%$, the capacity of RECC is higher by more than 50%. The curvature ductility of RECC is always higher than that of RC, even for highly reinforced sections, for example, if $\rho = 3\%$ ductility of RECC is higher by 40%.

REFERENCES

1 Li V.C., Wang S., Wu C.: Tensile Strain-Hardening Behavior of PVA-ECC. ACI Materials Journal, V. 98, No. 6, pp. 483-492, 2001.

2 Wang S., Li V.C.: Polyvinyl Alcohol Fiber Reinforced Engineered Cementitious Composites: Material Design and Performances. Proc. of International Workshop on HPFRCC Structural Applications, Hawaii, May 2005.

3 Bosco C., Carpinteri A., Debernardi P.G.: Minimum Reinforcement in High-Strength Concrete. Journal of Structural Engineering, V. 116, No. 2, pp. 427-437, 1990.

4 Fischer, G., and V.C. Li, "Influence of Matrix Ductility on the Tension-Stiffening Behavior of Steel Reinforced Engineered Cementitious Composites (ECC)," *ACI Structural J.*, Vol. 99, No. 1, pp. 104-111, 2002.